Journal of Catalysis **197,** 1–5 (2001)
doi:10.1006/jcat.2000.3088, available online at http://www.idealibrary.com on IDEAL®

PRIORITY COMMUNICATION

Atomic-Scale Structure of Co–Mo–S Nanoclusters in Hydrotreating Catalysts

J. V. Lauritsen,* S. Helveg,* E. Lægsgaard,* I. Stensgaard,* B. S. Clausen,† H. Topsøe,† and F. Besenbacher*,[1]

*CAMP and Institute of Physics and Astronomy, University of Aarhus, DK-8000 Aarhus C, Denmark; and †Haldor Topsøe Research Laboratories, Nymøllevej 55, DK-2800 Lyngby, Denmark

Received September 1, 2000; accepted September 15, 2000

By means of scanning tunneling microscopy (STM), it has been possible to obtain the first atomic-scale images of the Co–Mo–S structure present in hydrodesulfurization (HDS) catalysts. Information on the catalytically important edge structures has been obtained by synthesizing single-layer Co–Mo–S nanoclusters using the Au(111) herringbone structure as a template. It is observed that the presence of the Co promoter atoms causes the shape of the MoS_2 nanoclusters to change from triangular to hexagonally truncated. This change in morphology appears to be driven by a preference for Co to be located at the S-edge of MoS_2. The results also directly show that the presence of the Co atoms perturbs the local electronic environment of neighboring S atoms and this provides further insight into the effect of the promoter atoms.

Key Words: **scanning tunneling microscopy (STM); hydrodesulfurization; catalysis; Co–Mo–S; molybdenum disulfide.**

1. INTRODUCTION

The production of clean transport fuels by hydrotreating and especially deep hydrodesulfurization (HDS) has recently attracted increased attention due to the introduction of new environmental legislation regarding fuel specifications (1, 2). In order to meet the specifications there is an increased need to understand and improve HDS catalysts. Supported sulfides of Mo or W promoted with Co or Ni are applied widely for this service and they have been the subject of extensive investigations (3–6). It is generally accepted that the HDS activity is related to the presence of the so-called Co–Mo–S structures that consist of small MoS_2 or WS_2 clusters with promoter atoms located somewhere at the edges. However,the origin of the promoting role of Co or Ni and in particular the atomic-scale location of the promoter atoms in Co–Mo–S nanoclusters is still the subject of intense debate (3, 7, 8). This is related to the fact that the spectroscopic techniques, which have provided insight into the nature of the Co–Mo–S structures (see e.g. (9–15)), are not able to unequivocally map the real-space atomic structure.

To aid in the understanding of the industrial catalyst, new insight has been gained from studies of catalyst model systems applying surface science techniques (16–21). Recently, we have successfully used scanning tunneling microscopy (STM) to study the real-space structure of MoS_2 nanoclusters as a model system for HDS catalysts (21). However, the industrial catalysts are promoted with Co or Ni (3) and thus we focus in the present Communication on STM studies of the important Co–Mo–S structures. On the basis of atom-resolved STM images it is found that the presence of the Co atoms has a dramatic influence on the morphology of the MoS_2 structures. This is related to the observation that in Co–Mo–S, Co is only present at one type of MoS_2 edges, the so-called S-edge. Besides morphological and structural information, the results also provide direct information on changes in the local electronic environment of the sulfur atoms neighboring the Co edge-atoms. This insight may be important for understanding the promoting role. Finally, it is interesting that the STM results also reveal substitution of Co into the bulk structure of MoS_2 nanoclusters.

2. EXPERIMENTAL

The experiments are performed in an ultra-high-vacuum (UHV) chamber equipped with a unique home-built high-resolution STM, which has demonstrated the capability of providing atom-resolved images of a large variety of systems on a routine basis (22, 23). In this study, the Au(111) surface is chosen as a model substrate for two reasons. Gold is chemically rather inert such that the support interaction can be reduced. Furthermore, gold belongs to the class of metals, the surface of which reconstructs in the clean state. Specifically, the Au(111) has a characteristic

[1] To whom correspondence should be addressed. Fax: +45 8612 0740. E-mail: fbe@ifa.au.dk.

0021-9517/01 $35.00

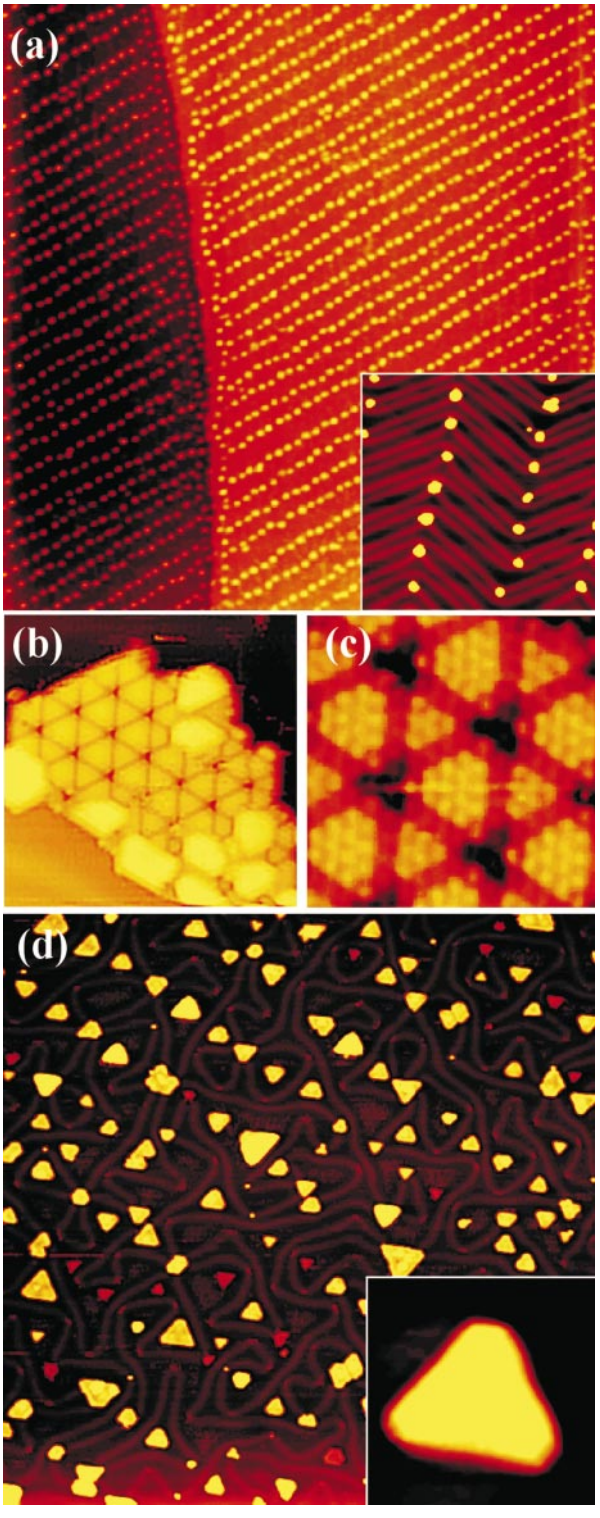

FIG. 1. (a) STM image (3435 Å × 3730 Å) of Co on Au(111). The inset (484 Å × 528 Å) shows a close-up of the ≈30 Å wide Co nanoclusters trapped in the elbow regions of the reconstructed Au(111) surface. (b) Large cobalt sulfide islands are present at the Au(111) step edges (152 Å × 186 Å). (c) Atom-resolved image of a cobalt sulfide island (50 Å × 54 Å). (d) STM image (969 Å × 1057 Å) showing Co–Mo–S nanoclusters on Au(111). The inset (68 Å × 74 Å) shows the predominant *hexagonally truncated* structure.

"herringbone" reconstruction pattern (24), which is ideal for providing nucleation sites for the deposited metal atoms (21) and thereby dispersing submonolayer amounts of Mo and Co into nanoclusters. Prior to the experiments, a Au(111) single-crystal surface is sputter-cleaned by 1.5 keV Ar ion bombardment followed by annealing to 900 K. In Fig. 1a is shown a large-scale STM image of Co deposited

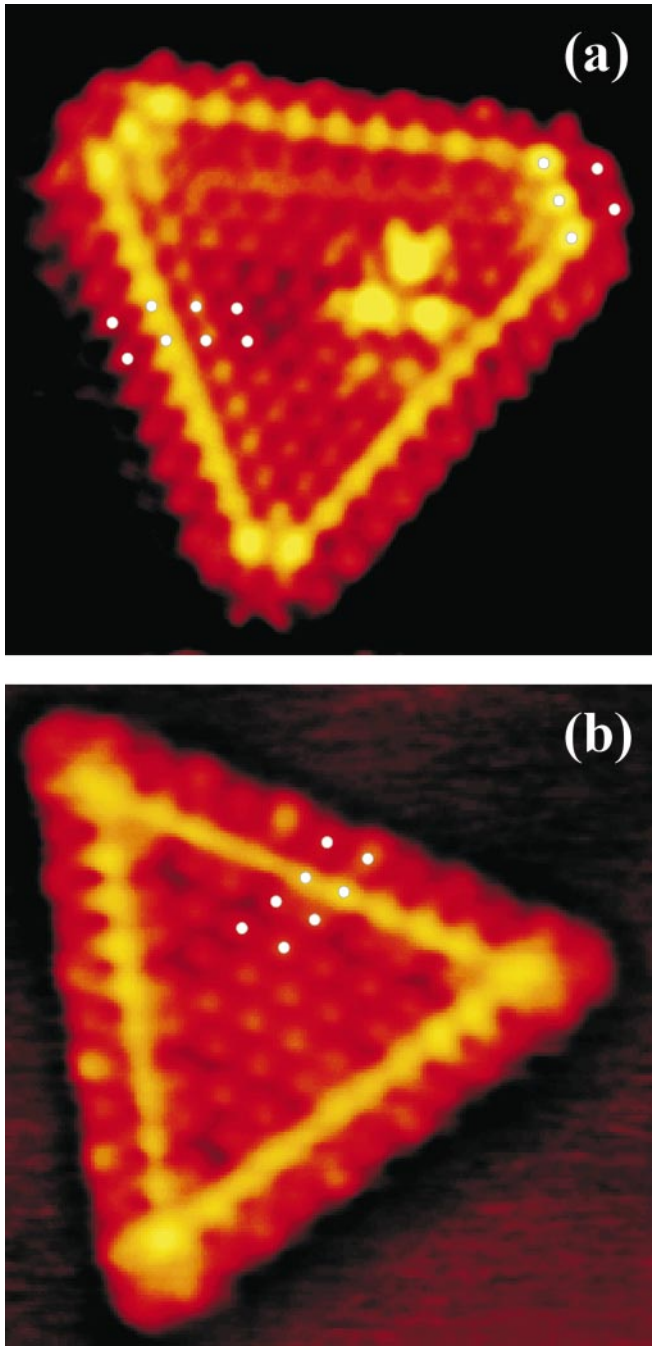

FIG. 2. (a) STM image (48 Å × 53 Å)of a single-layer Co–Mo–S nanocluster ($I_t = 1.95$ nA, $V_t = -430$ mV). (b) Triangular single-layer MoS_2 nanocluster (48 Å × 53 Å, $I_t = 1.28$ nA, $V_t = 5.2$ mV). In both images the small white dots illustrate the position of the protrusions.

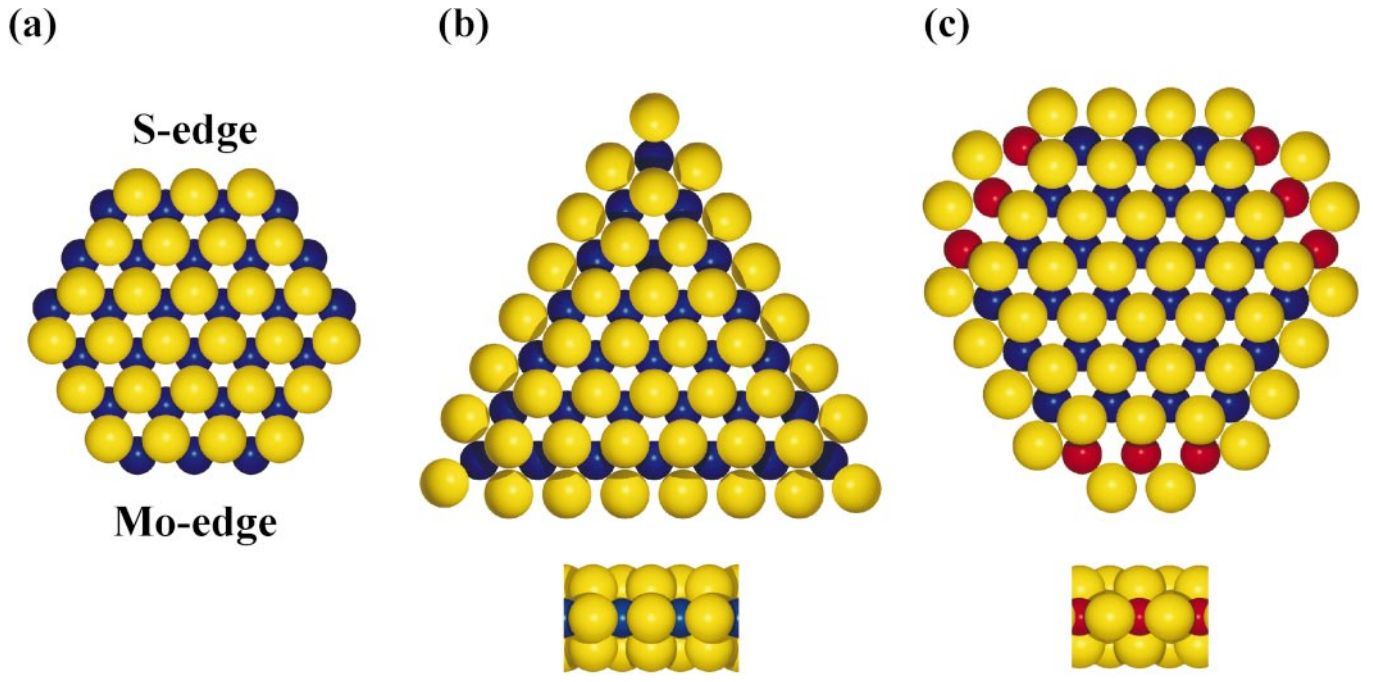

FIG. 3. (a) Ball model (top view) of a hypothetical bulk truncated MoS_2 hexagon exposing both Mo- and S-edges. (b) Triangular MoS_2 cluster exposing Mo-edges with edge sulfur atoms located out of registry with the basal plane. (c) Ball model of the proposed hexagonally truncated Co–Mo–S structures with Co fully substituted at the S-edges. Color code: Mo, blue; S, yellow; Co, red.

on Au(111). It is seen that the Co is deposited in regularly distributed Co nanoclusters located in the elbow regions of the Au(111) herringbone reconstruction. Similar findings were observed for the deposition of Mo on Au(111) (21).

We have observed that the choice of preparation procedure has a significant influence on the tendency to form Co–Mo–S nanoclusters (see below). This is not unexpected since changes in preparation parameters of the industrial CoMo-based catalysts also strongly influence the phase distribution (3). The preparation procedure described below was found to be particularly efficient in the synthesis of the bimetallic Co–Mo–S phase.

The idea is to form MoS_2 embryos followed by capping of these nanoclusters with Co to facilitate the addition of Co to the edges of MoS_2 nanocrystals. Initially, a core of sulfided Mo is produced by e-beam evaporating Mo onto the Au(111) surface while dosing gaseous H_2S. While maintaining the H_2S pressure (corresponding to a steady flux of $\sim 10^{16}$ molecules cm^{-2} s^{-1}), Co and Mo are subsequently co-deposited to provide an intermixed capping of the initial nanoclusters located on the reconstructed Au(111) template. The individual coverages for the deposited Mo and Co were estimated from STM images of the density of Mo and Co nanoclusters on Au(111) and found to be $\approx$10% for Mo and $\approx$4% for Co, respectively. This Co/Mo ratio is similar to that used in typical industrial catalysts. Finally, the intermixed CoMo metal sulfide nanoclusters are crystallized by postannealing at 673 K for 15 minutes, while keeping the H_2S background pressure.

3. RESULTS AND DISCUSSIONS

The co-deposition of Co and Mo in H_2S and subsequent crystallization is seen from the STM images to result in two coexisting phases (Fig.1): (i) large cobalt sulfide islands formed by step flow growth at the Au(111) step edges (23), and (ii) crystalline Co–Mo–S nanoclusters nucleated on the Au(111) terraces. In Fig. 1b is shown a large island grown at a Au(111) step edge together with an atom-resolved image (Fig. 1c). These large island structures are associated with a cobalt sulfide phase since similar structures are observed when *only* Co is deposited and subsequently sulfided on Au(111). Cobalt sulfide is known to exist in a variety of phases with different stoichiometries and crystallographic structures, e.g., Co_9S_8, but in view of the low catalytic significance of these cobalt sulfide structures (3), a detailed discussion will be postponed, to appear in a forthcoming publication.

We will thus in the following focus on the sulfided crystalline CoMo nanoclusters nucleated on the Au(111) terraces. One of the interesting new findings of the present study is that these nanoclusters have a *hexagonally truncated* shape (see Fig. 1d) as opposed to the *triangular* shape of the MoS_2 nanoclusters observed when only Mo was deposited and sulfided (Fig. 2b) (21). The observed morphology of the nanoclusters (the hexagons) is therefore attributed to the incorporation of cobalt in the MoS_2 structure, i.e., the formation of the Co–Mo–S phase.

Before we discuss these results further, a few basic structural features of MoS_2 will be mentioned. Molybdenum disulfide is a layered compound consisting of stacks of S–Mo–S slabs held together by van der Waals interactions. Each slab is composed of two hexagonal planes of S atoms and an intermediate hexagonal plane of Mo atoms, which are trigonal prismatically coordinated to the S atoms. The morphology of the MoS_2 nanocluster is determined by the relative stability of two types of edge terminations, i.e., the $(\bar{1}010)$S-edge and the $(10\bar{1}0)$Mo-edge. In Fig. 3a these two edge terminations are illustrated for a hypothetical MoS_2 cluster, where the edges are simple terminations of the bulk MoS_2 structure.

For the single-layer MoS_2 model system, the observed dominant triangular morphology (Fig. 2b) implies that one of the edge terminations is more stable than the other (21). Which edge termination is the most stable under sulfiding conditions has been inferred from a comparison of the atom-resolved STM images of MoS_2 nanocrystals with recent density functional theory (DFT) calculations (8). It was concluded that the edge termination is a Mo-edge and a possible model with one S atom per Mo-edge atom arranged in a reconstructed geometry is shown in Fig. 3b (21). However, another low-energy structure with S dimers at the Mo-edge may also be possible (8, 25). Which of the two models for the Mo-edge is most compatible with the observed STM images is currently being studied, and further details will be discussed elsewhere (26).

Atomically resolved STM images (Fig. 2a) of the Co–Mo–S nanoclusters reveal that the protrusions on the basal plane are arranged in a hexagonal symmetry with a lattice spacing of 3.15 ± 0.10 Å, and with an apparent height of 2.1 ± 0.3 Å. Before we proceed it is important to stress that low-bias constant current images reflect the local density of states (LDOS) at the Fermi level projected onto the position of the STM tip apex (27). The STM images thus in general represent a somewhat complicated convolution of the geometric and electronic structure. However, consistent with theoretical findings (26, 28) the protrusions can be associated with S atoms in the topmost sulfur layer. We thus conclude that the interior structure of the Co–Mo–S nanoclusters corresponds closely to that of single-layer MoS_2, with a hexagonal arrangement of the S atoms and an interatomic sulfur distance of 3.15 Å.

The observed hexagonal truncated morphology of the Co–Mo–S nanoclusters (Fig. 2a) implies that both edge terminations, i.e., S- and Mo-edges, must be present. The identity of the two edges is inferred from the high-resolution STM images of the Co–Mo–S edges. We find that the longer edges are identical with those observed for the triangular MoS_2 nanoclusters (21) with the protrusions being imaged *out* of registry with the protrusions on the basal plane. These edges are thus attributed to sulfided Mo-edges. Therefore, the Co promoter atoms appear to have little effect on the Mo-edges. From the symmetry of the crystal (Fig. 3a), the short edges are consequently attributed to S-edges. The result, that addition of cobalt stabilizes the S-edge relative to the situation of pure MoS_2 clusters, is in good agreement with the DFT calculations showing a preference for Co to be located at the S-edge (8). If we assume that the edge protrusions are associated with S atoms, a superimposed grid reveals that the S-edge atoms are close to being *in* registry with the S atoms in the basal plane. However, the S atoms appear to be displaced ~0.5 Å perpendicularly away from the edge compared to the bulk position.

Focusing on the short S-edges, the atomically resolved image in Fig. 2a shows that the brim structure behind the outermost row of sulfur atoms appears to be imaged more brightly, corresponding to an increase of the apparent height by ~1 Å relative to the S atoms on the basal plane. We suggest that this change in the LDOS is associated with the Co atoms present at the S-edges. The Co edge atoms appear to induce an enhanced electronic density at the nearby S atoms which consequently are imaged more brightly. It is possible that the perturbed electronic environment of the sulfur atoms neighboring the Co atoms may be a key to understanding the increased reactivity of the Co–Mo–S structures.

On the basis of the STM observations, we propose a structural model for Co–Mo–S, where the cobalt is substituted into Mo positions at the S-edge as depicted in the ball model in Fig. 3c. A *tetrahedral* environment of the Co is produced if the outermost S atoms are assumed to be bridge-bonded monomer sulfur atoms located in the plane of the Mo atoms. The proposed Co–Mo–S model is thus seen to have intrinsic undercoordinated metal sites, and from a catalytic point of view this may be an attractive situation enabling adsorption of the sulfur-containing reactants. The presence of the bridge-bonded monomer S atoms located in the Mo plane is consistent with an apparent outward displacement of the S atoms as observed in the STM images (Fig. 2a). The possibility that only a fraction of the Mo atoms on the S-edge are replaced by Co atoms seems unlikely on the basis of STM images of clusters with longer S-edges (up to six atoms wide). In these images, the periodicity along the S-edge is observed to be one lattice constant, indicating that the edge is fully substituted by Co.

In the literature many models for Co–Mo–S have been proposed (3, 4), but it is noteworthy that the present model is consistent with recent DFT calculations for the Co–Mo–S structure (8, 29) and with previously published spectroscopic results. From *in situ* extended X-ray absorption fine structure (EXAFS) (10, 14, 15, 30) the local environment of substituted Co atoms has been inferred. It was shown that the average distances from Co to the nearest atoms are $d_{\mathrm{Co–S}} \approx 2.2$ Å and $d_{\mathrm{Co–Mo}} \approx 2.9$ Å. Furthermore, the average coordination numbers were found to be $N_{\mathrm{Co–S}} = 5 \pm 1$ and $N_{\mathrm{Co–Mo}} \approx 2$. These coordination numbers are consistent with the fully substituted S-edge model shown in Fig. 3c.

In Fig. 2a we also observe three very bright spots (~1 Å higher than the neighboring basal plane S atoms) arranged in a triangular symmetry on the basal plane of the Co–Mo–S clusters. The three bright spots are found to occupy the positions of basal plane sulfur atoms. This suggests that a single Co atom has substituted a Mo atom in the basal plane metal lattice, and in analogy with the situation at the Co-substituted S-edges this induces an enhanced electron density at the three neighboring sulfur atoms. These Co species were not observed when Co was evaporated onto existing MoS_2 nanoclusters in the presence of H_2S. These are therefore quite different from the metallic (Ni) species observed recently (20) on top of the MoS_2 basal plane.

4. CONCLUSIONS

This Communication reports the synthesis of single-layer Co–Mo–S nanostructures, which are used as model systems for the industrial HDS catalysts. On the basis of atom-resolved STM images it is concluded that the Co atoms are located exclusively at the (1010) S-edges of the Co–Mo–S nanoclusters and there appears to be a preference for a full edge substitution by Co. The presence of the Co atoms is found to induce both structural, morphological, and electronic changes, and this insight may lead to an improved understanding of the promoting role of Co and Ni.

ACKNOWLEDGMENTS

We acknowledge stimulating discussions with J. K. Nørskov and M. Bollinger as well as financial support from the VELUX and Knud Højgaard Foundations. The Center for Atomic-scale Materials Physics (CAMP) is sponsored by The Danish National Research Foundation. J.V.L. and S.H. acknowledge support from the Danish Research Academy and the Interdisciplinary Center for Catalysis (ICAT). F.B. gratefully acknowledges the support from the Danish Technical Research Council and from the EU through the research training network contract entitled "Oxide surfaces—reactivity of clean and modified oxide surfaces."

REFERENCES

1. Knudsen, K. G., Cooper, B. H., and Topsøe, H., *Appl. Catal. A* **189**, 205 (1999).
2. Gosselink, J. W., *CaTTech* **4**, 127 (1998).
3. Topsøe, H., Clausen, B. S., and Massoth, F. E., *in* "Hydrotreating Catalysis, Science and Technology" (J. R. Anderson and M. Boudart, Eds.), Vol. 11. Springer-Verlag, Berlin, 1996.
4. Prins, R., *in* "Handbook of Heterogenous Catalysis" (G. Ertl, H. Knözinger, and J. Weitkam, Eds.), p. 1908, VHC Verlagsgesellschaft mbH, Weinheim, 1997.
5. Whitehurst, D. D., Isoda, T., and Mochida, I., *Adv. Catal.* **42**, 345 (1998).
6. Kabe, T., Ishihara, A., and Qian, W., "Hydrodesulfurization and Hydrogenation". Wiley, New York, 1999.
7. Hensen, E., and van Santen, R. A., *CaTTech* **3**, 86 (1998).
8. Byskov, L. S., Nørskov, J. K., Clausen, B. S., and Topsøe, H., *J. Catal.* **187**, 109 (1999).
9. Topsøe, H., Clausen, B. S., Candia, R., Wivel, C., and Mørup, S., *J. Catal.* **68**, 433 (1981).
10. Clausen, B. S., Lengeler, B., Candia, R., Als-Nielsen, J., and Topsøe, H., *Bull. Soc. Chim. Belg.* **90**, 1249 (1981).
11. Topsøe, N.-Y., and Topsøe, H., *J. Catal.* **84**, 386 (1983).
12. Boudart, M., Dalla Batta, R. A., Foger, K., Löffler, D. G., and Samant, M. G., *Science* **228**, 718 (1985).
13. Ledoux, M. J., Michaux, O., Agostini, G., and Panissod, P., *J. Catal.* **96**, 189 (1985).
14. Niemann, W., Clausen, B. S., and Topsøe, H., *Catal. Lett.* **4**, 355 (1990).
15. Louwers, S. P. A., and Prins, R., *J. Catal.* **133**, 94 (1992).
16. Salmeron, M., Somorjai, G. A., Wold, A., Chianelli, R. R., and Liang, K. S., *Chem. Phys. Lett.* **90**, 105 (1982).
17. Wiegand, B. C., and Friend, C. M., *Chem. Rev.* **92**, 491 (1992).
18. Muijsers, J. C., Weber, T., van Hardeveld, R. M., Zandbergen, H. W., and Niemantsverdriet, J. W., *J. Catal.* **157**, 698 (1995).
19. Gunter, P. L. J., Niemantsverdriet, J. W., Ribiero, F. H., and Somorjai, G. A., *Catal. Rev.-Sci. Eng.* **39**, 77 (1997).
20. Kushmerick, J. G., and Weiss, P. S., *J. Phys. Chem. B* **102**, 10094 (1998).
21. Helveg, S., Lauritsen, J. V., Lægsgaard, E., Stensgaard, I., Nørskov, J. K., Clausen, B. S., Topsøe, H., and Besenbacher, F., *Phys. Rev. Lett.* **84**, 951 (2000).
22. Lægsgaard, E., Besenbacher, F., Mortensen, K., and Stensgaard, I., *J. Microsc.* **152**, 663 (1988).
23. Besenbacher, F., *Rep. Prog. Phys.* **59**, 1737 (1996).
24. Barth, J. V., Brune, H., Ertl, G., and Behm, R., *Phys. Rev. B* **42**, 9307 (1990).
25. Byskov, L. S., Hammer, B., Nørskov, J. K., Clausen, B. S., and Topsøe, H., *Catal. Lett.* **47**, 177 (1997).
26. Bollinger, M., Jacobsen, K. W., and Nørskov, J. K., to be published.
27. Tersoff, J., and Hamann, D. R., *Phys. Rev. B* **31**, 805 (1985).
28. Altibelli, A., Joachim, C., and Sautet, C., *Surf. Sci.* **367**, 209 (1996).
29. Raybaud, P., Hafner, J., Kresse, G., Kasztelan, S., and Toulhoat, H., *J. Catal.* **190**, 128 (2000).
30. Bouwens, S. M. A. M., van Veen, J. A. R., Koningsberger, D. C., deBeer, V. H. J., and Prins, R., *J. Phys. Chem.* **95**, 123 (1991).